

# On the rapid forced reconnection in the Sun's corona for its localized heating

Abhishek Kumar Srivastava<sup>1</sup>, Petr Jelínek<sup>2</sup>, Sudheer K. Mishra<sup>1</sup>, Tanmoy Samanta<sup>3</sup>, Hui Tian<sup>3</sup>, Vaibhav Pant<sup>4</sup>, Pradeep Kayshap<sup>2</sup>, Dipankar Banerjee<sup>5</sup>, John Gerard Doyle<sup>6</sup>, Bhola N. Dwivedi<sup>1</sup>

<sup>1</sup>Department of Physics, Indian Institute of Technology (BHU), Varanasi-221005, India.

<sup>2</sup>University of South Bohemia, Faculty of Science, Institute of Physics, Branišovská 1760, CZ – 370 05 České Budějovice, Czech Republic.

<sup>3</sup>School of Earth and Space Sciences, Peking University, Beijing 100871, People's Republic of China.

<sup>4</sup>Centre for Mathematical Plasma Astrophysics (CmPA), KU Leuven, Celestijnenlaan 200B bus 2400, 3001, Leuven, Belgium.

<sup>5</sup>Indian Institute of Astrophysics, Kormangala, Bangalore, Karnataka, India.

<sup>6</sup>Armagh Observatory and Planetarium, College Hill, Armagh BT61 9DG, N. Ireland.

The million-degree hot solar corona maintains its high temperature and compensates for its radiative losses by continuously acquiring an energy flux of  $\approx 10^3 \text{ W m}^{-2}$ . Recent studies suggest that energy transport in the solar corona is associated with localized magnetic flux-tubes, which can channel various kinds of magnetohydrodynamic (MHD) waves and shocks as heating candidates. Dissipation of electric current via magnetic reconnection provides an alternate mechanism to heat the solar corona. However, there are various physical conditions that need to be established appropriately in the reconnection region to generate its high rate and subsequent energy release. Using multiwavelength imaging observations from the Atmospheric Imaging Assembly (AIA) onboard the Solar Dynamics Observatory (SDO), we present a novel physical scenario for the formation of a temporary X-point in the solar corona, where plasma dynamics is forced externally by a moving prominence. Natural diffusion was not predominant, however, a prominence driven inflow occurred firstly, forming a thin current sheet and enabling a forced magnetic reconnection at a considerably high rate. Observations vis-à-vis numerical model reveal that forced reconnection may rapidly and efficiently release energy in the solar corona to heat it locally even without establishing a significant and self-consistent diffusion region.

The Sun's corona continuously requires high amount of energy flux to compensate its radiative losses<sup>1</sup>. The major energy sources in the localized solar corona may be associated with magneto-hydrodynamic (MHD) waves and shocks<sup>1</sup>. However, global magnetic reconnection is a well known mechanism to explain various physical processes in the universe, and laboratory plasma experiments, e.g., solar and stellar flares, geomagnetic substorms and magnetosphere of planets, tokamak disruptions, high energy fusion experiments, etc<sup>9–12</sup>. In the astrophysical plasmas (e.g., solar corona), it is basically defined as a self-organization of the magnetic fields towards their more relaxed state and associated impulsive release of the stored magnetic energy<sup>13</sup>. In the solar corona, magnetic reconnection is considered as one of the major candidates to heat its atmosphere, and also to generate space weather candidates (e.g., flares and coronal mass ejections)

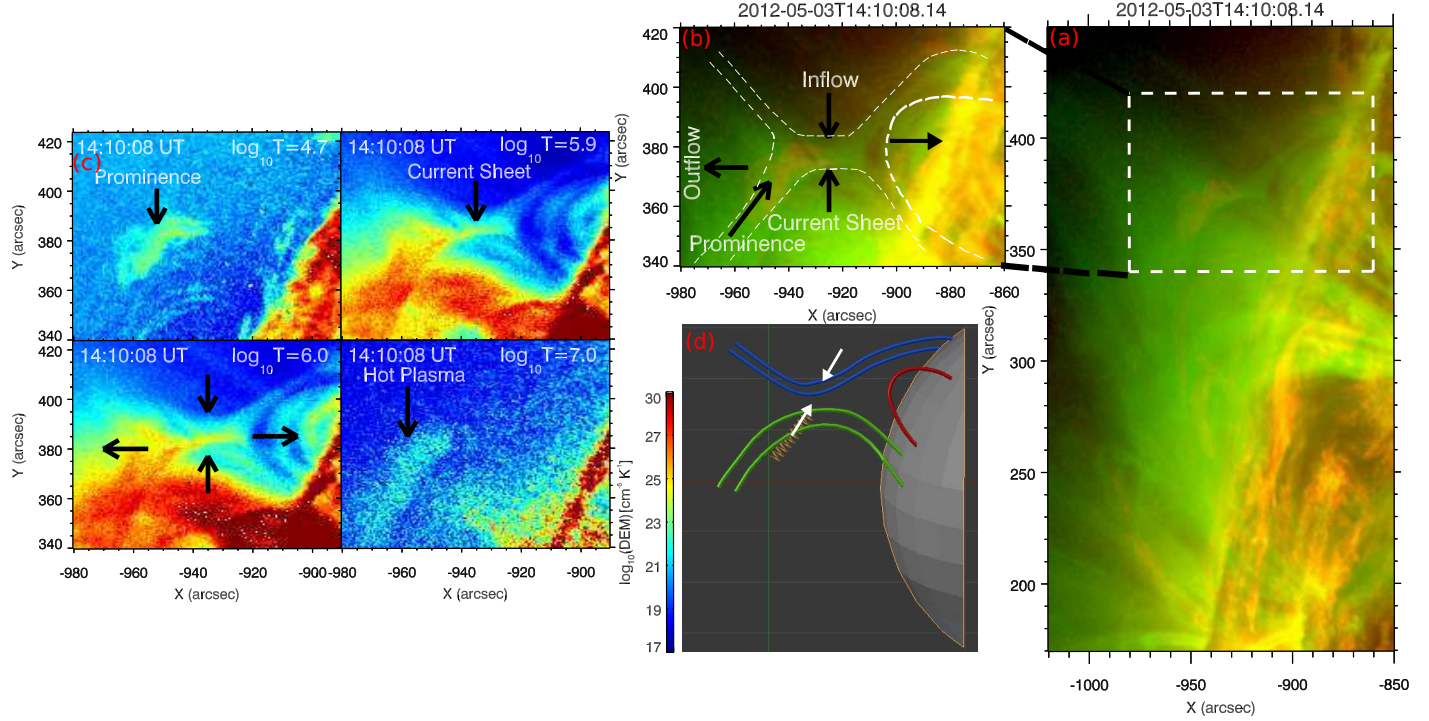
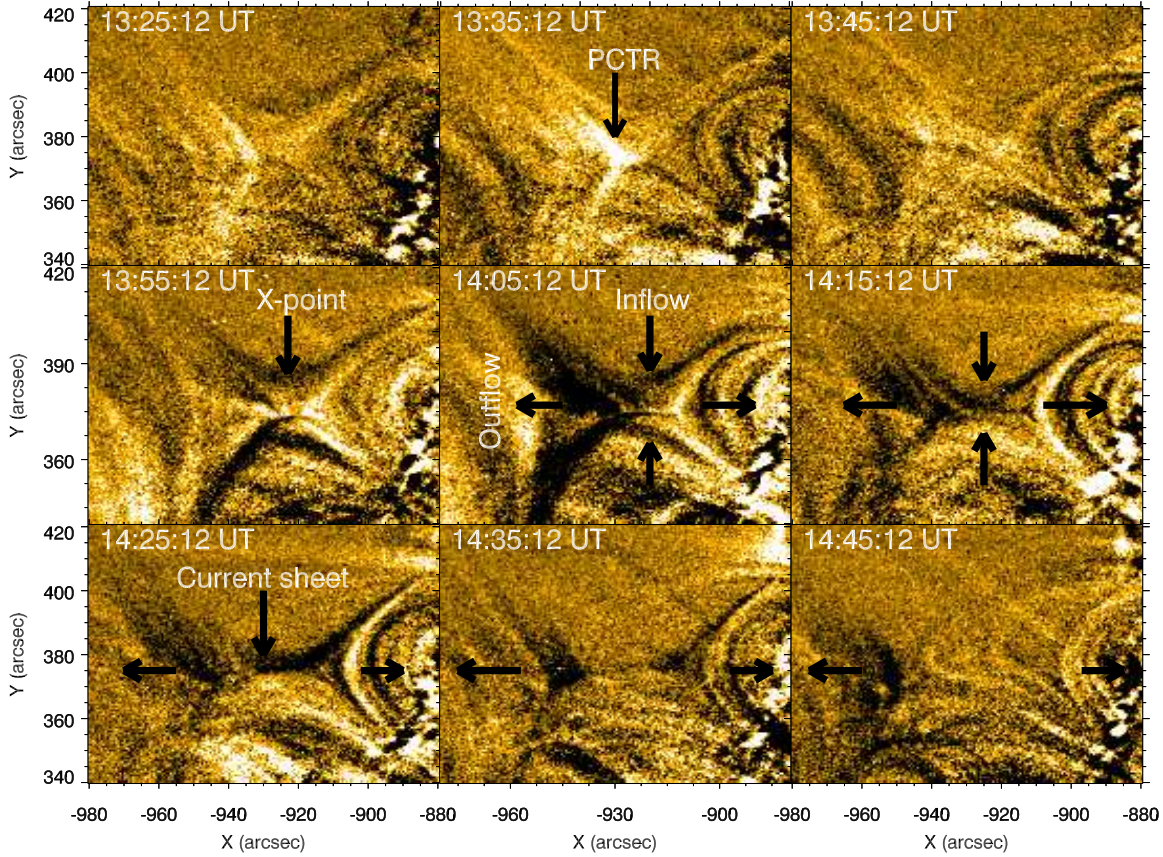


Fig. 1.— **Direct imaging of forced reconnection in the Sun's corona.** SDO/AIA imaging observations on 3rd May 2012 at 14:10:08 UT depict the formation of a temporary X-point and a forced reconnection region ('a'-'b'). Panel 'a' is the composite image of AIA 171 Å, 304 Å showing off-limb region. Panel 'b' is a zoomed view of the region of interest as shown by the dotted-black box in panel 'a'. The Differential Emission Measure (DEM)<sup>16</sup> maps for different temperature bins between  $\log T_e = 4.9$  and  $\log T_e = 7.0$  ('c') display that a prominence brings the overlying northward coronal magnetic field lines towards oppositely directed southward fields, and force externally the formation of an inflow at a X-point to trigger the reconnection. The schematic ('d') displays the creation of such forced reconnection epoch enabled by an external disturbance.



**Fig. 2.— Formation of X-point, and development of forced reconnection, inflow/outflow regions.** The running difference image sequence in the SDO/AIA 171 Å filter displays the motion of the prominence corona-transition region (PCTR) interface, which brings the southward branch of the coronal magnetic field towards the temporarily evolved X-point around 13:55 UT. The forced reconnection is subsequently triggered thereafter the initial onset of externally driven inflows. Plasma inflow occurs from the north-south direction (cf., image panel at 14:05 UT), and after the reconnection, the outflow is seen in the east-west direction (cf., panels during 14:05-14:35 UT). A dynamic current sheet is also formed during the forced reconnection process.

that can affect the Earth’s outer atmosphere, its satellite and communication system, etc<sup>9–12</sup>. However, the main issues of magnetic reconnection are still unsettled despite several novel discoveries both in theory and observations in a variety of astrophysical and laboratory plasmas, e.g., formation of current sheet, appropriate reconnection rate, establishment of natural diffusion regions and their physical properties, etc<sup>13–14</sup>. In the present letter, using multi-wavelength observations of the solar corona from the Atmospheric Imaging Assembly (AIA) onboard the Solar Dynamics Observatory (SDO) on 3 May 2012, we establish directly that forced reconnection at a considerably high rate can occur locally in its magnetized plasma (Fig. 1). It triggered in the corona when two oppositely directed magnetic field lines forming an X-point are perturbed by an external disturbance. This type of reconnection has only been reported in theory<sup>15</sup>, and has never been directly observed in the Sun’s large-scale corona. Although, an indirect signature of forced reconnection is claimed in the highly dynamic solar chromosphere at small spatial-scales for the release of tiny microflares<sup>16</sup>.

In the present scenario, the two branches of magnetic field lines are visible in the solar corona (cf., the black-dotted box in Fig. 1 ‘a’). The southward branch of the magnetic field envelopes a cool prominence, and is part of a large-scale closed field lines structure in the corona. The northward branch of the magnetic field is anchored at the limb, while its other end is open in the diffused corona. These two branches of large-scale coronal fields are separated by a low lying closed loop system with both foot-points anchored at the limb. The schematic (‘d’) clearly outlines the observed magnetic field configuration where the southward field, plus an embedded prominence (green) and open fields (blue) lie at the either sides of a low lying coronal loop system (red). The southward branch of the magnetic field lines is driven by the embedded prominence, moving towards the northward branch to form a temporary X-point. An inflow region is established at the X-point to enable the forced reconnection (Supplementary movies 1 & 2). The DEM map at different temperature bins between  $\text{Log } T_e=4.9$  and  $\text{Log } T_e=7.0$  (Fig. 1 ‘c’) and associated time-sequence (Supplementary movie 3; duration: 13:40 UT to 14:40 UT on 3 May 2012) also show that the cool prominence is enveloped by the southward branch of the hot and magnetized coronal plasma. The prominence plus the associated coronal field moves northward forming an X-point along with the northward branch of the magnetic fields. This enables **first** an inflow towards the evolved X-point in the corona and consequently forced magnetic reconnection begins. A dynamic current sheet is also formed during the reconnection process.

The sequence of difference images (Fig. 2; Supplemenatry movie 4) demonstrates that in the localized corona the inflow and associated X-point is created externally by the motion of the prominence around 13:55 UT. The hot plasma in the prominence corona-transition region (PCTR) also drifts towards the X-point, and brings the southward branch of the magnetic field near the inflowing northward magnetic field, triggering the forced reconnection. The bi-directional inflow starts from the north-south direction towards the X-point around 14:05 UT, and forced reconnection is triggered. Plasma outflows are also seen in the perpendicular east-west direction of the inflows along with the formation of a dynamic and elongated current sheet. It should be noted that the externally driven plasma inflows start first, and after the reconnection the outflows start. This is the key observational aspects of the forced reconnection. The time-distance



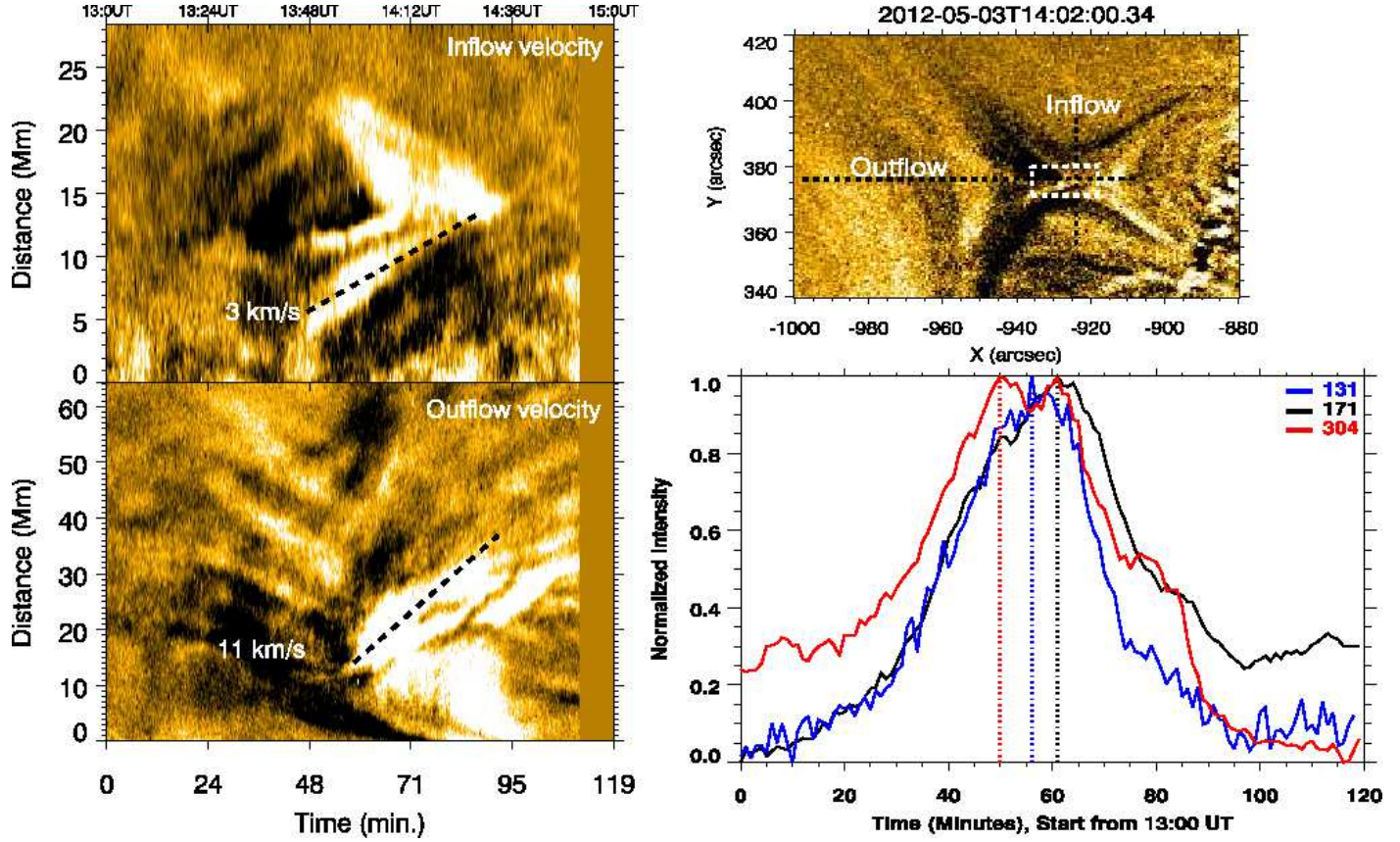


Fig. 3.— **The analyses of inflows, outflows, and nature of EUV emissions at the reconnection site.** The inflow and outflow plasma channels ('b') across the X-point have been selected to deduce the distance-time maps ('a') for estimating their speeds close to the X-point. The temporal variation of EUV plasma emissions (304 Å, 171 Å, 131 Å) has been measured to understand qualitatively the thermal response of the reconnection site.

maps (cf., Fig. 3 'a') along the inflow and outflow channels near the X-point (cf., Fig. 3 'b') show that the bidirectional inflow is followed by plasma outflow at the X-point. They occur respectively with speeds of  $\approx 3 \text{ km s}^{-1}$  and  $\approx 11 \text{ km s}^{-1}$  as detected close to the X-point. The outermost periphery of the reconnection region also shows some plasma outflows even before the start of the inflows, however, they are not directly linked to the response of the forced reconnection at the X-point and may be the stretching/re-arrangements of the outer coronal field lines during initiation of the reconnection. Therefore, we consider the pair of inflow and outflow due to forced reconnection which start close to the X-point. There is a time lag of few minutes between inflows and outflows that occur in the observed forced reconnection region at the X-point. The intensity at the X-point firstly peaks in the cool AIA 304 Å filter (Log  $T_e=4.7$ ) at  $\approx 13:50$  UT, which indicates that PCTR plasma segment first comes inside to form the X-point for forcing the reconnection. Once reconnection begins, the emission in the high temperature AIA filters 171 Å (Log  $T_e=5.9$ ), and 131 Å (Log  $T_e=6.9$ ) peak between  $\approx 14:00$  UT- $14:05$  UT (cf., Fig. 3 'c'). This exhibits a quick energy release at the X-point in  $\approx 10$  min time scale. Later, secondary post-reconnection processes are established at the X-point (e.g., dynamics and stretching of current sheet, outflows, cooling). The most significant aspect of this observed forced reconnection is its high rate ( $V_{in}/V_{out}$ ) ranging between  $\approx 0.27$ . A reconnection rate, as a dimensionless quantity, can be approximated by the ratio of inflow to the outflow speed<sup>14</sup>.

We developed a physical model of the observed forced reconnection by taking a weakly diverging, current-free equilibrium magnetic field embedded in a hydrostatic magnetohydrodynamic (MHD) solar atmosphere with an appropriate temperature profile<sup>17–18</sup>. We used an MHD code, known as FLASH<sup>19</sup> (Fig.4; see the details in Online-Appendix-I) to simulate the observed forced magnetic reconnection. The X-point is created in the equilibrium atmosphere along with an appropriate inclusion of the resistivity (Fig. 4, see details in Online-Appendix-I). The hydrostatic plasma equilibrium is perturbed by a localized velocity pulse set at the left side of the X-point, which resembles an external disturbance forcing the reconnection. The disturbance mimics an effect of a velocity field created by the moving prominence as seen in the observations. It is given as follows:

$$v_x = -A_0 \cdot \frac{x}{\lambda_y} \cdot \exp\left[-\frac{(x - L_p)^2}{\lambda_x}\right] \cdot \exp\left[-\frac{y^2}{\lambda_y}\right], \quad (1)$$

Here  $\lambda_x = 0.1 \text{ Mm}$  and  $\lambda_y = 0.1 \text{ Mm}$  are the width of the external disturbance ( $v_x$ ), which is a symmetric Gaussian-shaped velocity pulse in the vicinity of a null-point (Fig. 4). The  $x = 0.2 \text{ Mm}$  and  $y = 15 \text{ Mm}$  are the positions of the disturbance in the model corona. The amplitude  $A_0$  is fixed as  $0.1 \text{ Mm s}^{-1}$ .

The external disturbance propagates across the magnetic field lines as a fast magnetoacoustic perturbation, pushing the magneto-plasma system towards X-point from the left side (Fig. 4) with an effective plasma inflows of  $\approx 2.52 \text{ km s}^{-1}$ . This subsequently triggers the forced magnetic reconnection. After the reconnection of the field lines at the X-point, the magneto-plasma system is subjected to the outflows in the perpendicular direction with a speed of  $\approx 12.46 \text{ km s}^{-1}$ . This results in a reconnection rate of  $\approx 0.20$ , which lies in the observed range. This numerical simulation demonstrates that even if a sufficiently appropriate diffusion region is not created in the corona, an external driver can still trigger considerably rapid reconnection (cf., Supplementary movies 5 & 6). In the present numerical simulation, we have the value of resistivity,

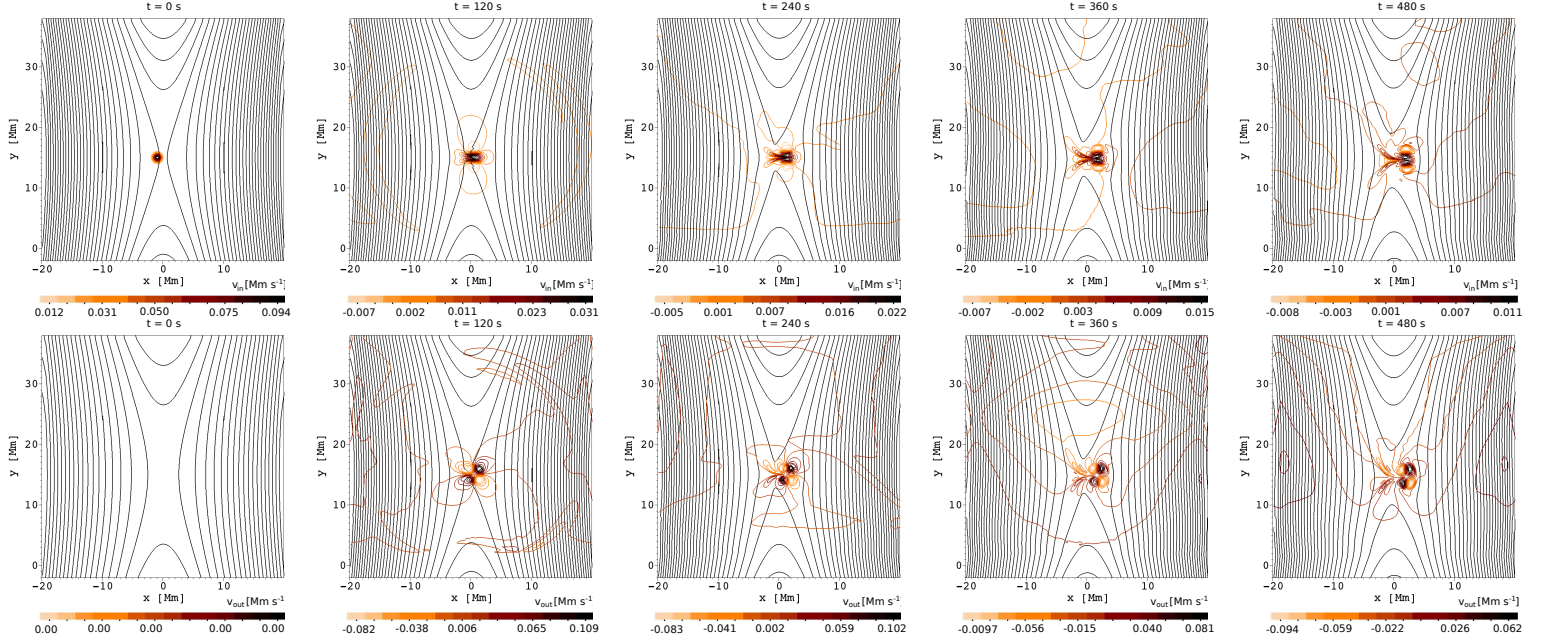


**Fig. 4.— Numerical model of the forced magnetic reconnection at X-point.** Using FLASH code, the X-point coronal magnetic field configuration has been reproduced on the observed spatial scales. An external disturbance is imposed on the left side of the X-point, which creates an average inflow of  $\approx 2.56 \text{ km s}^{-1}$  triggering the reconnection of the field lines. The plasma outflows with an average speed of  $\approx 12.46 \text{ km s}^{-1}$  has been generated during the reconnection in the perpendicular direction of the inflows. The simulated inflows, outflows, and the reconnection rate match with the observations of the forced reconnection. The various contours with different colours denote the velocities in units of  $\text{Mm s}^{-1}$ . The top and bottom rows display respectively inflow and outflow velocity contours around X-point as overplotted on the reconnection region. The total duration of the reconnection process is  $< 10$  min in the simulation, which match with the duration of physical processes (inflows, reconnection heating as well as outflows) as established initially in the reconnection region between 13:55 UT and 14:05 UT (cf., Fig. 3 ''c').

which is sufficient to start physical reconnection, and the numerical effects are almost negligible. The other aspect is that we observe the reconnection very shortly after the start of our simulation confirming that the tiny numerical resistivity does not affect the physical forced reconnection. The reconnection occurs in the present system, where the ratio between the length and width of the current sheet is high.

To show the physical significance of the observed and modelled forced reconnection in the corona, we performed a parametric study in the numerical simulation on the same spatio-temporal scales as we see in observations. We decrease the resistivity at the X-point and increase the strength of the external disturbance (cf., Fig. S2.1 in Online-Appendix-II). This indicates that we control more the magnetic reconnection in the localized corona by an external disturbance. Reconnection occurs by producing a pair of plasma inflow and outflow, as well as the formation of a thin current sheet in each case. The estimated reconnection rate increases even after the decrement of the resistivity at the X-point as the external velocity pulse forcing the reconnection increases gradually (cf., Figs. S2.2 & S2.3 in Online-Appendix-II). Therefore, the forced reconnection is established here as a significant mechanism for the rapid release of the magnetic energy in the corona even when natural diffusion does not play an important role.

The evolution of the hot plasma is visible in the form of outflowing plasma streaks (Fig. 1 'c'), as well as high temperature emissions (AIA 131 Å,  $\text{Log } T_e=7.0$ ) at the reconnection site (Fig. 3 ''c'). However, the bulk energy release in the present case is not as prominent as seen in typical flare sites<sup>20</sup>. This region is a quiescent loop system in the corona where there is no flare related energy stored in magnetic fields. In spite of this, we observe evidence of the evolution of heating in the localized corona due to the forced reconnection.

Although the issue related to the magnetic reconnection (e.g., rate, magnitude of diffusivity and resistivity, plasma and magnetic field structuring, amount of stored and released energy) are still highly debated, there is evidence for the unambiguous presence of this physical process which makes it as one of the key mechanisms for coronal heating and plasma eruptions<sup>21–24</sup>. The directly and firstly observed forced reconnection in the present paper does not require the establishment of large magnetic diffusivity (see the Online-Appendix-II) in the localized corona as required for the normal reconnection. The specific morphological (a typical length-scale of reconnection) as well as typical magnetic fields also do not influence it significantly. This forced magnetic reconnection does not build a large energy component, however, its stored amount in coronal fields can be liberated over appropriate time-scales typical for the localized heating and transient processes<sup>11,25</sup>. The highly dynamic and complex solar corona can be inevitably subjected to such forced reconnection at diverse spatio-temporal scales when external disturbances act on the partially or fully established reconnection regions, thus making it a significant physical mechanism for a variety of dynamical plasma processes in the solar corona<sup>27</sup>. These first observational clues to the forced reconnection can also be extended to the laboratory plasma, where it can be employed to generate the "green energy" and to constrain the behaviour of highly diffusive plasmas<sup>20</sup>.

1. Withbroe, G. L. & Noyes, R. W. Mass and energy flow in the solar chromosphere and corona. *Ann.*



- Rev. Astron. Astrophys.* **15**, 363-387 (1977).
2. Wedemeyer-Bohm, S. et al. Magnetic tornadoes as energy channels into the solar corona. *Nature* **486**, 505-508 (2012).
  3. Jess, D. et al. Alfvén waves in the lower solar atmosphere. *Science* **323**, 1582-1585 (2009).
  4. De Pontieu, B. et al. Chromospheric Alfvénic waves strong enough to power the solar wind. *Science* **318**, 1574-1577 (2007).
  5. McIntosh, S. et al. Alfvénic waves with sufficient energy to power the quiet solar corona and fast solar wind. *Nature* **475**, 477-480 (2011).
  6. Martínez-Sykora, J. et al. On the generation of solar spicules and Alfvénic waves. *Science* **356**, 1269-1272 (2017).
  7. Srivastava, A. K. et al. High-frequency torsional Alfvén waves as an energy source for coronal heating, *Nature SR* **7**, 43147 (2017).
  8. Srivastava, A. K. et al. Confined pseudo-shocks as an energy source for active Sun’s corona, *Nature Astr.*, <http://dx.doi.org/10.1038/s41550-018-0590-1> (2018).
  9. Cargill, P.J. & Klimchuk, J.A. Nanoflare heating of the corona revisited. *Astrophys. J.* **605**, 911-920 (2004).
  10. Klimchuk, J.A. Key aspects of coronal heating. *Phil. Trans. R. Soc. A.* **373**, 20140256 (2015).
  11. Shibata, K. & Magara, T. Solar flares: Magnetohydrodynamic processes. *Liv. Rev. Sol. Phys.* **8**, 6 (2011).
  12. Schwenn, R. Space weather: The solar perspective. *Liv. Rev. Sol. Phys.* **3**, article id. 2, 72 pp (2006).
  13. Yamada, M., Kulsrud, R. & Ji, H., Magnetic reconnection, *Rev. Mod. Phys.* **82**, 603-664 (2010).
  14. Priest, E.R. & Forbes, T.G. *Reconnection of Magnetic Fields: Magnetohydrodynamics and Collisionless Theory and Observations* (Cambridge Univ. Press, 2007).
  15. Jain, R., Browning, P. & Kusano, K., Solar coronal heating by forced magnetic reconnection: Multiple reconnection events. *Phys. Plasmas* **12**, 012904-012904-12 (2005).
  16. Jess, D.B., Mathioudakis, M., Browning, P.K., Crockett, P.J. & Keenan, F. P. Microflare activity driven by forced magnetic reconnection. *Astrophys. J.* **712**, L111-L115 (2010).
  17. Vernazza, J. E., Avrett, E. H. & Loeser, R. Structure of the solar chromosphere. III-Models of the EUV brightness components of the quiet-sun. *Astrophys. J.* **45** (suppl.), 635-725 (1981).
  18. Jelínek, P., Karlický, M. & Murawski, K. Electric current filamentation at a non-potential magnetic null-point due to pressure perturbation. *Astrophys. J.* **812**, 105.
  19. Fryxell, B. et al. FLASH: An adaptive mesh hydrodynamics code for modeling astrophysical thermonuclear flashes. *Astrophys J.* **131** (suppl.), 273-334 (2000).
  20. Su, Y., Veronig, A. M., Holman, G. D., Dennis, B. R., Wang, T., Temmer, M., & Gan, W. Imaging coronal magnetic-field reconnection in a solar flare. *Nature* **500**, 489-493 (2013).
  21. Li, L., Zhang, J., Peter, H., Priest, E., Chen, H., Guo, L., Chen, F., & Mackay, D. Magnetic reconnection between a solar filament and nearby coronal loops. *Nature* **540**, 847-851 (2016).
  22. Xue, Z., Yan, X., Cheng, X., Yang, L., Su, Y., Kliem, B., Zhang, J., Liu, Z. Bi, Y., Xiang, Y., Yang, K., & Zhao, L. Observing the release of twist by magnetic reconnection in a solar filament eruption. *Nature Communications* **7**, 11837 (2016).
  23. Lin, J., Ko, Y.-K., Sui, L., Raymond, J. C., Stenborg, G. A., Jiang, Y., Zhao, S., & Mancuso, S. Direct

observations of the magnetic reconnection site of an eruption on 2003 November 18. *Astrophys. J.* **622**, Issue 2, article id. 1251 1264, (2005).

24. Sui, L., & Holman, G. D. Evidence for the Formation of a Large-Scale Current Sheet in a Solar Flare. *Astrophys. J.* **596**, L251-L254 (2003).

25. Vekstein, G. Forced magnetic reconnection. *J. Plasma Phys.* **83**, 205830501, 32 (2017).

26. Yamada, M., Yoo, J., Jara-Almonte, J., Ji, H., Kulsrud, R.M., & Myers, C.E. Conversion of magnetic energy in the magnetic reconnection layer of a laboratory plasma. *Natur Comm.* **5**, 4774 (2014).

27. Potter, M.A.; Browning, P.K., and Gordovskyy, M. Forced magnetic reconnection and plasmoid coalescence: I - MHD Simulations. *Astron. Astrophys.* <https://arxiv.org/pdf/1901.02392.pdf> (2019).

\*Correspondence and request for materials/on-line materials should be addressed to Dr. A.K. Srivastava (Email: asrivastava.app@iitbhu.ac.in).

### Acknowledgment

AKS acknowledges UKIERI project grant, and the Advanced Solar Computational & Analyses Laboratory (ASCAL). P. J. acknowledges support from Grant 16-13277S of the Grant Agency of the Czech Republic. AKS, DB, and BND acknowledge the Indo-US (IUSSTF/JC-2016/011) for the support in their research. TS and HT are supported by NSFC grants 41574166 and 11790304 (11790300). Armagh Observatory and Planetarium is grant-aided by the N. Ireland Department of Communities. JGD acknowledges the DJEI/DES/SFI/HEA Irish Centre for High-End Computing (ICHEC) for the provision of computing facilities and support. JGD also thanks STFC for PATT T&S and the SOLARNET project which is supported by the European Commission's FP7 Capacities Programme under Grant Agreement number 312495 for T&S.

---

### Data Availability Statement:

The data that support the plots within this paper and other findings of this study are available from the corresponding author upon reasonable request.

### List of On-line Materials:

(i) **Online-Appendix-I:** A concise theoretical details of the magnetohydrodynamic (MHD) model of the forced magnetic reconnection used in the present work. Details of perturbation, numerical setting & methods, model of the solar magnetic field etc are described in this appendix.

(i) **Online-Appendix-II:** Comparisons of the role of resistivity as well as strength of external disturbances on the rate of the forced magnetic reconnection at coronal X-point have been discussed.

**(ii) Supplementary Movie 1:** Movie shows the evolution of the forced magnetic reconnection in the off-limb large-scale corona.

**(iii) Supplementary Movie 2:** Movie shows the evolution of the inflows, outflows and formation of the current sheet in the reconnection region.

**(iv) Supplementary Movie 3:** DEM movie shows the motion of an external driver (prominence), inflows, outflows, and currentsheet. It demonstrates the multi-temperature view of the forced reconnection.

**(v) Supplementary Movie 4:** Movie shows the complete evolution of the forced magnetic reconnection in the localized corona in difference map sequence in SDO/AIA 171 Å.

**(vi) Supplementary Movies 5 & 6:** Movies collectively show the evolution of the forced magnetic reconnection in the model solar atmosphere driven by an external disturbance. This mimics the observations of the forced reconnection in the solar corona.